Colloid Polym Sci 273:252–256 (1995)

ORIGINAL CONTRIBUTION

A. Bot
R.P.C. Schram
G.H. Wegdam

Brillouin light scattering from a biopolymer gel: hypersonic sound waves in gelatin

Received: 2 May 1994
Accepted: 17 August 1994

A. Bot (✉)
Unilever Research Laboratorium
Vlaardingen
Olivier van Noortlaan 120
3133 AT Vlaardingen, The Netherlands

R.P.C. Schram · G.H. Wegdam
Van der Waals-Zeeman Laboratory
University of Amsterdam
Valckenierstraat 65
1018 XE Amsterdam, The Netherlands

Abstract Rayleigh–Brillouin light scattering experiments were performed on gelatin gels in order to obtain the (hypersonic) sound velocity and sound attenuation as a function of gelatin concentration. The results show that in the high frequency regime there is a strong coupling in the gel between the dynamics of the network and that of the fluid. The network sound velocity varies with $\phi^{1/2}$. Sound attenuation increases with increasing gelatin concentration.

Key words Gels – gelatin – Rayleigh–Brillouin light scattering – hypersonic sound – Marqusee – Deutch hydrodynamical model

Introduction

Many of the static and dynamic properties of the gelatin network have been studied extensively using scattering techniques. Static light scattering experiments have revealed the phase diagram and the kinetics of gelation [1,2]. From small-angle neutron scattering experiments and static light scattering experiments the dynamic mesh size of the network has been found to be typical of the order of several nanometers [3,4]. Correlation spectroscopy reveals that two types of diffusion take place in the gel: a fast mode due to diffusion of individual gelatin coils and a slow mode due to diffusion of groups of entangled coils [5].

A question that has not been studied is to what extent the dynamics of the network and that of the solvent are coupled in a gelatin gel. A suitable technique to study this question is Brillouin light scattering (see, e.g., Berne and Pecora [6]). With this technique it is possible to study phonon-like thermal excitations in the gel. Marqusee and Deutch have proposed a hydrodynamical model that describes the dynamics of a gel [7]. They state that if there is a weak coupling between the dynamics of the network and that of the solvent, two sound modes can be observed: one carried by the network and one by the solvent, neither with much concentration dependence. On the other hand, if there is a strong coupling between the dynamics of the network and that of the solvent (i.e., the gelatin and the aqueous buffer solution), a single sound mode is predicted with a propagation frequency that is strongly dependent on the concentration. Two cases for this strong coupling limit can be distinguished. In one case there is only frictional coupling and sound modes in the network are dampened by the presence of the fluid (no elastic coupling), in the other case a sound wave in the network can also lead to sound waves in the fluid or vice versa (elastic coupling).

We have performed Rayleigh–Brillouin light scattering experiments on gelatin gels to obtain the hypersonic sound velocity and sound attenuation as a function of the gelatin concentration. Data obtained have been interpreted in terms of a hydrodynamical model proposed by Marqusee and Deutch [7] and compared with results of earlier work on gels. We have applied data analysis techniques which

were developed for the analysis of Rayleigh–Brillouin spectra of fluids, and which have proven to be very sensitive tools in the study of Brillouin lines [8].

Rayleigh–Brillouin light scattering

In a light scattering experiment an incoming light wave with $k_i = |\mathbf{k}_i| = 2\pi/\lambda_i$ is partially scattered by local fluctuations in the dielectric constant of the sample. Here, k_i is called the (angular) wavevector and λ_i is the wavelength of the incoming beam. Part of the scattered light, characterized by $\mathbf{k}_f$, is analyzed. The vectors $\mathbf{k}_i$ and $\mathbf{k}_f$ determine the scattering angle θ and the scattering geometry. The wavevector $\mathbf{k} = \mathbf{k}_f - \mathbf{k}_i$ is associated with the fluctuations that cause scattering. Since $|\mathbf{k}_i| \approx |\mathbf{k}_f|$, it follows that

$$k = |\mathbf{k}| = \frac{4\pi n}{\lambda_i} \sin\frac{\theta}{2}, \tag{1}$$

where n is the refractive index of the scattering medium.

The frequency distribution of light is changed by the scattering process. If the spectrum of the incoming beam is a narrow single peak, the spectrum of the scattered light may have completely different characteristics. In a typical dynamic light scattering experiment on a liquid or a dense gas one observes the so-called Rayleigh–Brillouin triplet: a symmetric spectrum around the (angular) frequency of the incoming light, $\omega_i = 2\pi c/\lambda_i$, consisting of a central or Rayleigh line and two shifted or Brillouin lines. Here, c is the speed of light.

The triplet is described in hydrodynamic fluctuation theory as the sum of Lorentzians and a pair of associated asymmetrical terms. Line widths, positions and intensities in the spectrum are determined by the thermodynamic and transport properties. Furthermore, in the limit of small k, shifts are proportional to k and widths are proportional to k^2. The Brillouin peaks can be interpreted as Doppler shifted lines, and the shift with respect to the Rayleigh line is proportional to the product of adiabatic velocity of sound and wavevector [6]. A hydrodynamical model for gels predicts similar behavior for the Brillouin line shift and line width [7]. The linear k dependence of the shift has been tested by Mallamace et al. [9] in methyl(2-methylpropenoate) + 1,2-ethanediyl(2-methylpropenoate) gels.

Experiment and data analysis

Experiment

A Coherent CR-4 argon-ion laser was used operating single mode at wavelength of 514.5 nm and an output power of approximately 200 mW. The main part of the beam was focused in a 10 mm cuvette. Light scattered at an angle of 90° was analyzed by a single-pass Fabry-Perot interferometer. The interferometer was equipped with flat plates, one of which could be translated piezoelectrically. A Centronic Q4249B photomultiplier served as a detector and the signal was fed into a Burleigh–DAS1 data acquisition and stabilization system. A smaller part of the beam was diverted and was used as a signal to monitor the instrumental profile of the interferometer simultaneously.

In each experiment three orders of the interferogram were monitored. The first order consisted predominantly of the trigger pulse, and was used for stabilization purposes by the data acquisition system. The second and third order of the spectrum were used to determine the free spectral range ω_{FSR} of the interferometer. The free spectral range of the interferometer was $1.35 \cdot 10^{11}$ rad·s^{-1}, the finesse was typically 40, and the contrast was typically 900. More details on the equipment can be found elsewhere [10].

The gelatin used was obtained from Gelatin Delft, The Netherlands (Bacteriological gelatin, Bloom strength 245, weight loss on drying 11.8%, ash content 0.78%). The gelatin gels were prepared by dissolving the gelatin in a pH = 5.6 potassium hydrogen phthalate + sodium hydroxide buffer while stirring and heating for approximately 10 min, and then leaving it for 1 h at 60 °C. As a germicide 0.02% w/w sodium azide was added. Gels were prepared with gelatin weight fractions $\phi = 0.01$, 0.04, 0.10, 0.14, and 0.20. Light scattering spectra were measured at room temperature (21.5 ± 0.5 °C). A single spectrum was taken in 15 min for gels with the most pronounced Brillouin lines, and in other gels in typically 1 h. For every gel the spectrum was followed for a day.

The refractive index measurements for the gelatin solutions were made with a Zeiss 51592 refractometer. No effect of ageing on the refractive index was observed.

Data analysis

An experimentally obtained light scattering spectrum is convolution of the instrumental profile of the experimental set-up, and an intrinsic line shape due to the processes which are probed:

$$I_{exp}(k,\omega) = I_{ins}(\omega) * I(k,\omega), \tag{2}$$

where * denotes the convolution and $I(k,\omega)$ represents the Fourier–Laplace transform of the dielectric autocorrelation function. For $I(k,\omega)$ we have used the sum of an unshifted Lorentzian and two pairs of shifted Lorentzians with corresponding asymmetrical line shapes (cf. Schram et al. [11]):

$$I(k,\omega) \propto Re \sum_j \frac{A'_j z'_j - A''_j(\omega - z''_j)}{z'^2_j + (\omega - z''_j)^2}, \tag{3}$$

where A_j' and A_j'' are amplitudes of the symmetrical Lorentzian and that of its associated asymmetrical line. For an unshifted Lorentzian $A_j'' = 0$. The parameters z_j' and z_j'' denote the width (HWHM) and shift of the Lorentzian under consideration. Most of the parameters in this fit were used to obtain a good fit for the wings of the Rayleigh line, which allowed us to determine reliable parameters for the Brillouin lines. The instrumental profile is given by the Airy formula [12]. For an Airy profile the intensity at $\pm \omega_{FSR}/2$ is still over 0.1% of the intensity at the maximum for a finesse of 40. Since the Rayleigh line is much more intense than the Brillouin lines in these experiments (see Fig. 1), a background (relative to the Brillouin intensity) is caused at $\omega = \pm \omega_{FSR}/2$. One way to decrease this background would be to increase the finesse of the interferometer, or alternatively to use a multi-pass interferometer and thus increase the contrast. Adjusting the free spectral range of the interferometer does not decrease this background contribution [13].

The presence of the background is a problem since the Rayleigh line is so much more intense than the Brillouin lines (see Fig. 1), a fitting procedure will optimize essentially the Rayleigh line only. This can be circumvented by analyzing the current autocorrelation spectrum $\omega^2 I_{exp}(k,\omega)$ rather than the spectrum $I_{exp}(k,\omega)$ itself (see Fig. 2). However, the presence of the additional background due to the instrumental profile results in an unphysical current autocorrelation spectrum which diverges rather than vanishes for large ω. To prevent this we need to subtract the background contribution. By taking the intensity halfway two orders of the interferogram as the background and subtracting that from the spectrum, we essentially modify the instrumental profile by performing a background correction [14]. This procedure solves the background problem in the data analysis.

Using this background correction, we fitted the current autocorrelation spectrum by Eq (3) multiplied by ω^2. We fitted $\omega^2 I_{exp}(k,\omega)$ until fits were satisfactory on visual inspection. Our automatic fitting procedure made use of a simple fitting routine (see, e.g., Press et al. [15]). An example of $\omega^2 I_{exp}(k,\omega)$ and a typical fit are shown in Fig. 2.

The data analysis techniques described above were developed for the analysis of Rayleigh–Brillouin spectra of fluids, and have proven to be very sensitive tools in the study of phonon lines shifted with respect to a dominant elastic peak [13].

Fig. 1 Rayleigh-Brillouin light-scattering $I_{exp}(k,\omega)$ of a $\phi = 0.10$ gelatin gel. The spectrum is dominated by the Rayleigh line

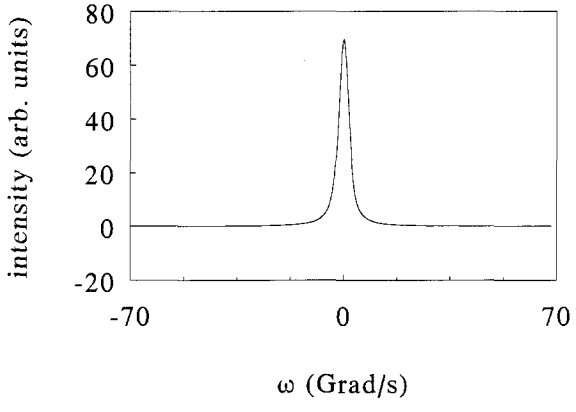

Fig. 2 Current autocorrelation spectrum $\omega^2 I_{exp}(k,\omega)$ for a $\phi = 0.10$ gelatin gel. The Brillouin lines are clearly visible

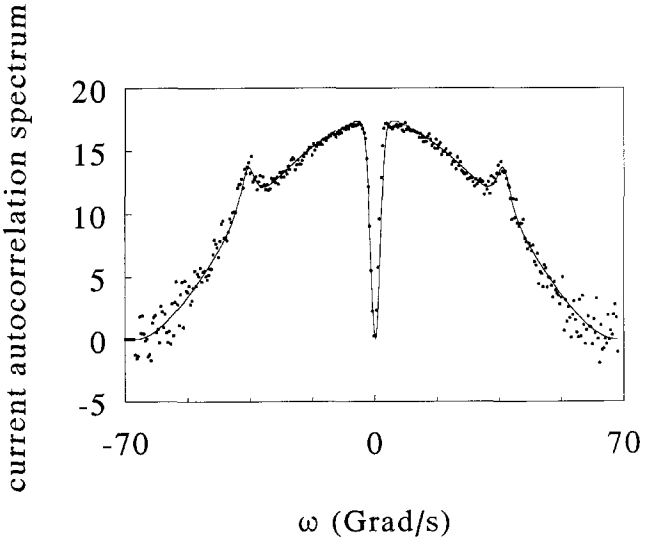

Results

We have obtained hypersonic sound velocities and attenuations from fits like that in Fig. 2 by dividing the observed Brillouin line shift by the wavevector, and by dividing the observed line width by the square of the wavevector. The value of the wavevector has been corrected for the concentration dependence of the refractive index n, which we found to be represented by the relation $n = 1.3350 (\pm 0.0003) + 0.1794(\pm 0.0018) \pm \phi$ at 25 ± 0.5 °C.

From Fig. 3, we can see that the velocity of sound of the gel increases slightly with increasing gelatin concentration. Each point represents an average over several spectra taken at different ageing times, since we did not observe a trend in the Brillouin shifts due to ageing of the gelatin gel.

The data in Fig. 3 may be compared with a hydrodynamical model by Marqusee and Deutch [7]. We

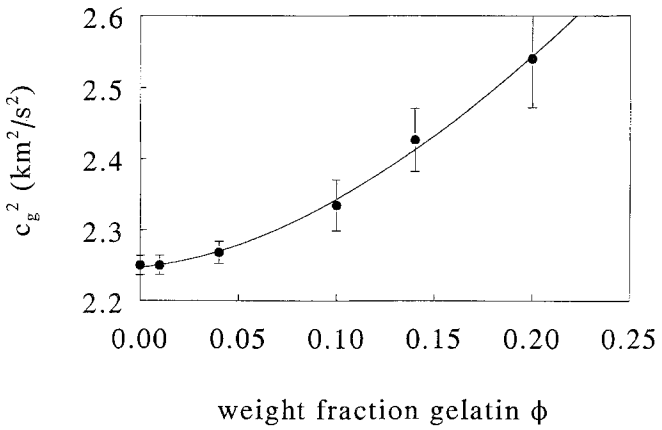

Fig. 3 Square of the observed hypersonic sound velocity as a function of gelatin weight fraction ϕ

denote the high-frequency velocities of sound in the uncoupled fluid, in the uncoupled network, and in the gel by c_f, c_n, and c_g respectively. Analogously, we denote the densities in fluid, network and gel by ρ_f, ρ_n and ρ_g respectively. Furthermore, we assume explicit concentration dependencies for these densities (see Table 1) and the network velocity of sound: $c_n = \phi^{1/2} v_n$. Here, v_n is the hypothetical sound velocity for pure gelatin. In the limit of strong frictional coupling of the Marqusee–Deutch model, we then obtain the expression

$$c_g^2 = \frac{1}{\rho_g}(\rho_f c_f^2 + \rho_n v_n^2 \phi + 2\sqrt{\lambda \rho_n \rho_f} c_f v_n \phi^{1/2}) \quad (4)$$

In other words, for low concentrations the high-frequency sound velocity of the gel is determined mainly by the sound velocity of the fluid, and only corrections originate from the presence of the network. The parameter λ in Eq. (4) gives the elastic coupling between fluid and network, varying between 0 (weak elastic coupling) and 1 (strong elastic coupling). In a fit of the data according to Eq. (4) we found $\lambda = 0.333$. The resulting fitting parameters have been listed in Table 1, the fit has been plotted in Fig. 3. It can be seen that the fit gives a qualitatively good description of the data.

In Table 2 we have listed results for the observed Brillouin line width divided by k^2. It can be seen that the damping of the sound mode initially stays roughly constant and then increases with increasing gelatin concentration. However, since the errors in the Brillouin line widths are larger (because these widths are much more sensitive to the exact fit to the wing of the Rayleigh line than the Brillouin line shifts), the data should be considered not accurate enough to test the Marqusee–Deutch theory for the Brillouin line width under the present experimental conditions.

Table 1 Fitting parameters used in Eq. (4). Densities were extrapolated from ref. [2].

Parameter	Value
c_f	1499 m/s
v_n	2143 m/s
λ	0.333
ρ_g	$1 + 1.48\phi$ g/cm^3
ρ_f	$1 - \phi$ g/cm^3
ρ_n	2.48ϕ g/cm^3

Table 2 Experimental results for the square of the hypersonic sound velocity (c_g^2) and sound mode damping (Γ_{FWHM}/k^2) as a function of gelatin weight fraction ϕ.

ϕ	c_g^2 (km^2/s^2)	Γ_{FWHM}/k^2 (mm^2/s)
0	2.250 ± 0.014	3.8 ± 0.7
0.01	2.250 ± 0.014	3.1 ± 0.7
0.04	2.268 ± 0.016	3.9 ± 0.9
0.10	2.335 ± 0.036	3.7 ± 1.0
0.14	2.427 ± 0.045	5.8 ± 1.4
0.20	2.541 ± 0.068	6.6 ± 1.5

Discussion and conclusions

To our knowledge only three other Brillouin light scattering studies on biopolymers have been made. In the first study, Hosea et al. [16] followed the Brillouin shift as a function of temperature and used that to identify the glass transition of sucrose. The nature of their study is therefore quite different from that of ours. In the other two studies, the dynamics of wet spun films of oriented polymer chains has been investigated as a function of polymer concentration in the film: Tao et al. [17] studied Na- and Li-DNA films and Lee et al. [18] studied films of the polydisaccharide hyaluronic acid. Although these studies are more related to the present subject, both are dealing with oriented chains and film-shaped samples, which hampers comparison with the present results.

In order to compare our results with those of other works, we had better look at a study on a synthetic polymer gel in water. For example, Ng and Li [19] have studied the Brillouin line shift and line width for poly(ethenol) and poly(chloroethene) gels as a function of polymer concentration. They found that their results are consistent with a model that predicts a sound mode that is characteristic of the average elastic properties of the gel, or in other words with the strong friction limit of the Marqusee–Deutch theory. To get a satisfactory agreement between theory and experiment, they assume a velocity of sound for the network that is proportional to $\phi^{1/2}$ [19, 20].

Our results indicate that the dynamics of a gelatin gel is also described by the Marqusee–Deutch model in the limit of strong friction. Like Ng and coworkers [19, 20], we find that the network velocity of sound is proportional to $\phi^{1/2}$, and that the agreement between theory and experiment is very good. Remarkably, the explicit concentration dependence assumed above for the network (longitudinal) high-frequency sound velocity is in agreement with the observed concentration dependence of the low-frequency shear modulus of gelatin, G', which is proportional to the square of the gelatin concentration [21]: the low-frequency (shear) velocity of sound must be proportional to $\phi^{1/2}$ then, since it is proportional to $(G'/\rho_n)^{1/2}$ and since the network density is proportional to ϕ. (It is interesting to note that from scaling theory it is found that for swollen gels that $G \propto \phi^{2.25}$ for a given solvent and fixed functionality [22]. The power 2.25 is slightly higher than the value 2 usually attributed to gelatin [21]. As a consequence, the resulting power for the concentration dependence of the network sound velocity would be somewhat higher than 0.5)

It is now tempting to explain the $\phi^{1/2}$ dependence of the network sound velocity obtained from these experiments in terms of the structure of the network. If we assume that the gelatin network may be treated in the same way as the aerogel network studied by Courtens et al. [23], we can write

$$c_n \propto \phi^{\left(\frac{D_{ac}}{\delta}-1\right)/(3-D_{ac})} \quad (5)$$

In this equation D_{ac} is the acoustical fractal dimension of the network, which is a probe of the connectivity of the network, and δ is the spectral dimension, which defines the phonon density of states in terms of a power of ω. If we use the elastic scalar prediction for the spectral dimension, $\delta = 4/3$, which is consistent with the results for the silica aerogels [23], we obtain $D_{ac} = 2$. In this way it would be possible to probe the connectivity of the network, using the ϕ dependence of the high-frequency velocity of sound. However, the validity of this analysis has not been tested for gelatin. Especially the fractal nature of the network on short scales has not been demonstrated, and can only be established by extensive wavevector dependent measurements. This is a task well beyond the aim of this study.

The values obtained for the sound velocity indicate that the bulk modulus of the gel is dominated by the bulk modulus of the fluid. Similar values for the sound velocity in gelatin were obtained in ultrasonic experiments (see, e.g., Reddy [24]).

Finally, we would like to add that a combination of our data analysis methods with multi-pass interferometric techniques should make it possible to study some systems where the presence of a very strong Rayleigh line has previously prevented analysis of Brillouin light scattering data.

Acknowledgement R.P.C.S. and G.H.W. acknowledge support from the Foundation for Fundamental Research of Matter (FOM) and the Netherlands Organization for Research (NWO).

References

1. Bohidar HB, Jena SS (1993) J Chem Phys 98:3568–3570; 8970–8977
2. Bohidar HB, Jena SS (1994) J Chem Phys 100:6888–6895
3. Pezron I, Djabourov M, Leblond J (1991) Polymer 32:3201–3210
4. Djabourov M, Bonnet N, Kaplan H, Favard N, Favard P, Lechaire JP, Maillard M (1993) J Phys II France 3:611–624
5. Herning T, Djabourov M, Leblond Takerkart G (1991) Polymer 32:3211–3217
6. Berne BJ, Pecora R (1976) Dynamic Light Scattering, Wiley, New York
7. Marqusee JA, Deutch JM (1981) J Chem Phys 75:5239–5245
8. Wegdam GH, Bot A, Schram RPC, Schaink HM (1989) Phys Rev Lett 63:2697–2700
9. Mallamace F, Micali N, Vasi C, Bansil R, Pajevic S, Sciortino F (1992) J Phys II France 2:2081–2088
10. Wegdam GH, Schaink HM (1989) Phys Rev A 40:7301–7310
11. Schram RPC, Wegdam GH, Bot A (1991) Phys Rev A 44:8062–8071
12. Born M, Wolf E (1980) Principles of Optics, Sixth Edition, Pergamon, Oxford
13. Bot A, Schaink HM, Schram RPC, Wegdam GH (1991) J Phys Chem 95:4673–4679
14. Schram RPC, Wegdam GH, Bot A (1994) J Phys Chem 98:3139–3147
15. Press WH, Teukolsky SA, Vetterling WT, Flannery BP (1992) Numerical Recipes in Fortran, Second Edition, Cambridge University Press, Cambridge
16. Hosea TJC, Ng SC, Oates CG (1990) Food Hydrocolloids 4:137–147
17. Tao NJ, Lindsay SM, Rupprecht A (1988) Biopolymers 27:1655–1671
18. Lee SA, Flowers MR, Oliver WF, Rupprecht A, Lindsay SM (1993) Phys Rev E 47:677–683
19. Ng SC, Li Y (1993) J Phys II France 3:1241–1245
20. Ng SC, Gan LM, Li Y, Chieng TH (1994) J Phys II France 4:715–722
21. Te Nijenhuis K (1981) Colloid Polym Sci 259:522–535
22. De Gennes PG (1979) Scaling Concepts in Polymer Physics, Cornell University Press, Ithaca, p 157
23. Courtens E, Pelous J, Phalippou J, Vacher R, Woignier T (1987) Phys Rev Lett 58:128–131
24. Reddy MA (1980) J Acoust Soc Ind 8:24–31